Progress In Electromagnetics Research, PIER 70, 257–267, 2007

COUNTER-PROPAGATING ENERGY-FLOWS IN NONLINEAR LEFT-HANDED METAMATERIALS

L. Chen, W. Ding, X.-J. Dang, and C.-H. Liang

National Key Laboratory of Antennas and Microwave Technology
Xidian University
Xi'an 710071, China

Abstract—A peculiarity of counter-propagating energy-flows in nonlinear left-handed metamaterials (LHMs) is investigated for the case when the frequency of fundamental wave is in the negative-index range and second-harmonic wave is in the positive-index range. Based on the electromagnetic theory, the comparisons of Manly-Rowe relations for nonlinear materials and process of second-harmonic generation under phase-matching condition in LHMs and RHMs are shown separately. That a surface of nonlinear left-handed metamaterials operates as an effective mirror which reflects the energy in form of second harmonics is demonstrated. Numerical results of fundamental and second-harmonic field intensity distributions are in agreement with theoretical results.

1. INTRODUCTION

The electromagnetics of complex media has been the subject of interest for many researchers in the past several decades. In recent years, the topic of metamaterials, i.e., artificial materials synthesized by embedding specific inclusions in host media, has increasingly received a renewed attention due to the interest in man-made complex materials that may possess negative real permittivity and permeability in a certain range of frequency. In 1967, Veselago postulated theoretically a material in which both permittivity and permeability were assumed to have negative real values, and he analyzed plane wave propagation in such a medium, which he called "left-handed metamaterials" [l]. The vectors $\boldsymbol{K}$, $\boldsymbol{E}$, $\boldsymbol{H}$ form a left-handed set in such materials, so many exciting and unusual properties are expected: negative refractive index, the anomalous Snell's law, opposite Doppler effect and backward Cherenkov radiation cone et al. [2–6]. The study of linear wave

propagation and the linear properties of left-handed materials (LHM) is a major subject of research in this field, and it is indeed the case when both the magnetic permeability and the dielectric permittivity of the material do not depend on the intensity of the electromagnetic field. However, the future efforts creating tunable structures in which the field intensity changes the transmission properties of the composite structure would require the knowledge of nonlinear properties of such metamaterials, which may be quite unusual.

In 2003, Zharov et al. proposed the possibility to control the effective parameters of the metamaterial using nonlinearity [7]. In [8], they showed that arrays of wires and split-ring resonators embedded into a nonlinear dielectric or diodes inserted in the SRRs will create hysteresis-type nonlinear magnetic response. An important property of subwavelength imaging with opaque left-handed nonlinear lens was discussed in [9], such lens can transfer the near-field image into second-harmonic frequency domain, and overcome absorption and dissipative losses which are the most challenging problems of perfect lens. The second-harmonic generation in left-handed slabs in the constant-pump approximation were analyzed in [10] which revealed the existence of multistable nonlinear effects.

In this paper, the counter-propagating energy-flows in a lossless nonlinear LHM slab beyond the constant-pump approximation is analyzed. Firstly, Manly-Rowe relations and the basic coupled-mode equations for LHM are studied. Secondly, energy conversion process and spatial distribution of forward-propagating wave of fundamental frequency and backward-propagating wave of second harmonics under phase-matching condition are investigated separately in a slab of a finite thickness and a semi-infinite slab. During this process some peculiarly properties are obtained. While numerical results of fundamental and second-harmonic field intensity distribution in a LHM slab and a RHM slab of finite thickness are given separately. Finally, the second harmonics under phase-mismatching condition are investigated to demonstrate the importance of the phase-matching condition.

2. BASIC COUPLED-MODE EQUATIONS AND MANLEY-ROWE RELATIONS FOR LOSSLESS NONLINEAR LHM

2.1. Mode and Basic Equations

We consider a lossless nonlinear slab with a thickness of L shown in Fig. 1, and assume the frequency of the fundamental wave ω is in the LHM domain ($\mu(\omega) < 0$, $\varepsilon(\omega) < 0$), the frequency of second

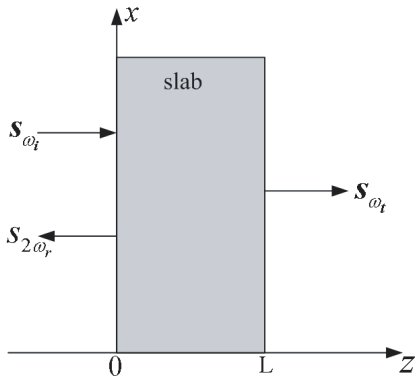

Figure 1. Geometry of the second-harmonics process for a finite-thickness slab of a lossless nonlinear LHM slab.

harmonic wave 2ω is in the RHM domain ($\mu(\omega) > 0,\ \varepsilon(\omega) > 0$) [9]. An incident flow of fundamental plane wave s_ω at ω propagates along the z-axis. For the double negative reason, the fundamental wave vector k_ω is opposite to s_ω along the $-z$-axis. According to phase-matching condition $k_{2\omega} = 2k_\omega$, and for the double positive reason, the second-harmonic wave vector $k_{2\omega}$ is equidirectional to $s_{2\omega}$, also along the $-z$-axis. The incident plane wave is described as:

$$H(\omega, z) = \frac{1}{2} h(\omega, z) e^{j\phi_\omega} \tag{1}$$

where ϕ_ω is the wave phase, and $h(\omega, z)$ is the field amplitude.

Taking the process of the second-harmonic generation into account, it contains the process to generate the wave of the sum frequency 2ω and the process to produce the wave of the difference frequency ω. And the nonlinear response is primarily associated with the magnetic component of the waves [8]. The general coupled-mode equations describing the simultaneous propagation of two harmonics in the lossless LHM can be written as follow:

$$\nabla^2 H(2\omega, z) + \varepsilon(2\omega)\mu(2\omega)\frac{(2\omega)^2}{c^2} H(2\omega, z) = -\frac{(2\omega)^2}{c^2}\chi_{2\omega} H^2(\omega, z) \tag{2}$$

$$\nabla^2 H(\omega, z) + \varepsilon(\omega)\mu(\omega)\frac{(\omega)^2}{c^2} H(\omega, z) = -\frac{(\omega)^2}{c^2}\chi_{2\omega} H(2\omega, z) H^*(\omega, z) \tag{3}$$

Here, $\chi_{2\omega}$ is the effective nonlinear susceptibility [9]:

$$\chi_{2\omega} = \frac{(\pi a^2)^3 \omega_0^4}{c^3 d^3 U_c R_d \omega^2} \left(\frac{\omega_0^2}{\omega^2} - 1\right)^{-2} \tag{4}$$

where a is the radius of the resonator rings, R_d is the differential resistance of the diode at zero voltage. U_c is the diode parameter defined from the current-voltage characteristics of the diode which we take in the form $I = I_0(e^{U/U_c} - 1)$.

Although the slab is lossless, the nonlinear response will generate the coupling among the waves. Refer to the harmonic waves of frequency of ω and 2ω, part of energy is coupled to the other harmonic components and vice versa. So $H(\omega, z)$ and $H(2\omega, z)$ are the functions of the coordinates. Under the small-signal condition, according to the perturbation theory, the amplitudes of the harmonic waves are assumed to vary slowly in both space and time, and then we can get the basic coupled-mode equations:

$$\frac{dH(2\omega, z)}{dz} = j\frac{2\varepsilon(2\omega)\omega^2}{k_{2\omega}c^2}\chi_{2\omega}H^2(\omega, z)\exp(-j\Delta kz) \tag{5}$$

$$\frac{dH(\omega, z)}{dz} = j\frac{\varepsilon(\omega)\omega^2}{2k_{\omega}c^2}\chi_{2\omega}H(2\omega, z)H^*(\omega, z)\exp(j\Delta kz) \tag{6}$$

where $\Delta k = k_{2\omega} - 2k_{\omega}$, the asterisk stands for the complex conjugation.

2.2. Manley-Rowe Relations for LHM

Like other nonlinear systems, the sum of the energy is constant in the process of the wave coupling in nonlinear LHM systems. By the basic coupled-mode equations, the sum of (5) multiplied by $\frac{k_{2\omega}}{\varepsilon(2\omega)}H^*(2\omega, z)$ and the complex conjugation of (6) multiplied by $\frac{k_{\omega}}{\varepsilon(\omega)}H(\omega, z)$ is found as:

$$\frac{k_{\omega}}{\varepsilon(\omega)}\frac{d|H(\omega, z)|^2}{dz} + \frac{k_{2\omega}}{2\varepsilon(2\omega)}\frac{d|H(2\omega, z)|^2}{dz} = 0 \tag{7}$$

The Poynting vector is expressed as:

$$s = \frac{k_{\omega}}{\varepsilon(\omega)}|H(\omega)|^2 \tag{8}$$

Considering the phase-matching condition $k_{2\omega} = 2k_{\omega}$, we take $\mu(\omega) = -\mu(2\omega)$, and $\varepsilon(\omega) = -\varepsilon(2\omega)$. The integral of (7) is obtained:

$$|H(\omega, z)|^2 - |H(2\omega, z)|^2 = c \tag{9}$$

Equation (9) is another expression of Manley-Rowe relations for LHM, c is an integration constant. However, Manley-Rowe relations for the RHM [11]:

$$|H(\omega, z)|^2 + |H(2\omega, z)|^2 = c \tag{10}$$

From (9) and (10) we can get that the difference between the squared amplitudes in LHM remains constant, but the sum of the squared amplitudes in RHM is constant. The difference of spatial distribution of forward-propagating wave of fundamental frequency and backward-propagating wave of second harmonics between LHM and RHM is decided by the distinction between (9) and (10), as schematically shown in Fig. 2.

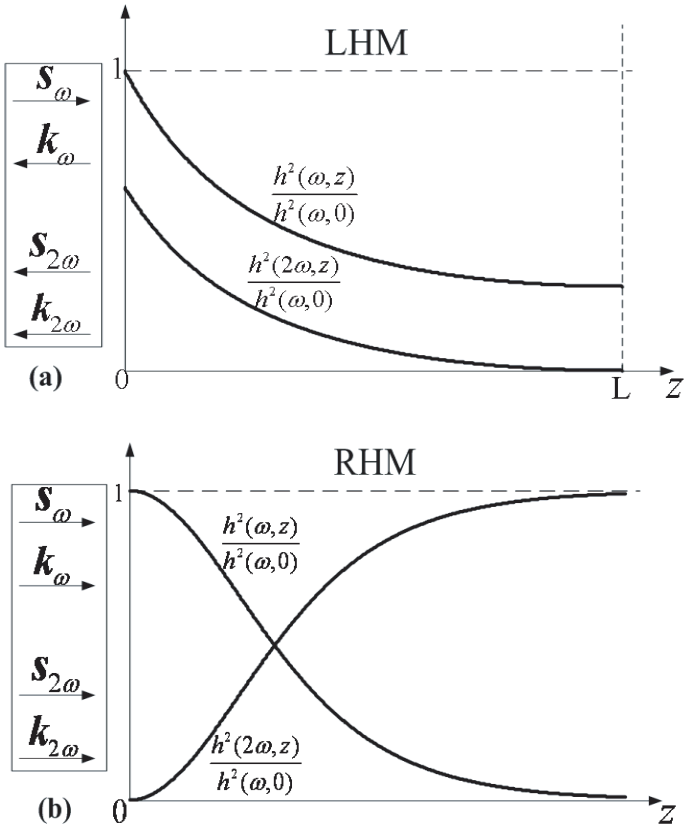

Figure 2. The process of second-harmonic generation under the phase-matching condition, and the energy spatial distribution of fundamental wave and second-harmonic wave normalized by $h^2(\omega, 0)$ versus z. (a) In LHM (b) In RHM.

3. SECOND-HARMONIC GENERATION IN A NONLINEAR LHM SLAB

The plane wave of fundamental frequency ω propagating in the lossless nonlinear LHM slab generates second-order nonlinear magnetization intensity constantly. It results in the source of the second-harmonic wave which propagates along the opposite direction to the surface of the slab $z = 0$. Conservation of energy in the slab is expressed as:

$$s(2\omega, z) + s(\omega, z) = s(2\omega, 0) + s(\omega, 0) \tag{11}$$

$$|H(\omega, z)|^2 - |H(2\omega, z)|^2 = |H(\omega, 0)|^2 - |H(2\omega, 0)|^2 \tag{12}$$

Under the phase-matching condition, substitution of (1) to (5) yields:

$$\frac{dh(2\omega, z)}{dz} = -\frac{\varepsilon(2\omega)\omega^2}{k_{2\omega}c^2}\chi_{2\omega}[h^2(2\omega, z) + h^2(\omega, 0) - h^2(2\omega, 0)] \times \exp\left[j\left(2\phi_\omega - \phi_{2\omega} - \frac{\pi}{2}\right)\right] \tag{13}$$

Except for the exponential terms the remains are all real in equation (13), we obtain $2\phi_\omega - \phi_{2\omega} - \pi/2 = 0$. It indicates that the phase difference between fundamental wave and second-harmonic wave remains constant $\pi/2$ in LHM, in accord with that in RHM.

Because of the boundary conditions $h(2\omega, L) = 0$, using the integral $\int \frac{dx}{a^2+x^2} = \frac{1}{a}\arctan\frac{x}{a}$, we solved (13):

$$h(2\omega, z) = \sigma \tan[\sigma\kappa(L - z)] \tag{14}$$

where $\sigma = \sqrt{h^2(\omega, 0) - h^2(2\omega, 0)}$, $\kappa = \varepsilon(2\omega)\omega^2\chi_{2\omega}/k_{2\omega}c^2$. Expression (14) is the field distribution of second-harmonic wave in the slab. The field distribution of fundamental wave is derived from substitution of (14) to (12):

$$h(\omega, z) = \sigma \sec[\sigma\kappa(L - z)] \tag{15}$$

By equations (14) and (15), the energy spatial distribution normalized by $h^2(\omega, 0)$ in LHM is shown in Fig. 2(a). The energy of two waves decreases along the z-axis, and that of the second-harmonic wave decrease to zero at $z = L$. The difference of them remains constant anywhere in the LHM slab.

Then consider the case of a semi-infinite LHM slab at $z > 0$, the thickness $L \to \infty$. With phase-matching condition, the energy of fundamental wave converts into that of second-harmonic wave constantly. Because their energy fluxes are guided along the opposite direction, both waves disappear at $z \to \infty$ and their amplitudes

are equal at $z = 0$. Taking into account the boundary condition, $h(2\omega, 0) = h(\omega, 0)$, 100% of the incident fundamental wave converts into the reflected second-harmonic wave. It is demonstrated that the surface of nonlinear LHM can operates as an effective mirror which reflects all the energy in the form of second harmonics. Solving equation (13) over again, field distribution expression is obtained:

$$h(2\omega, z) = h(\omega, z) = \frac{h(\omega, 0)}{1 + h(\omega, 0)\kappa z} \tag{16}$$

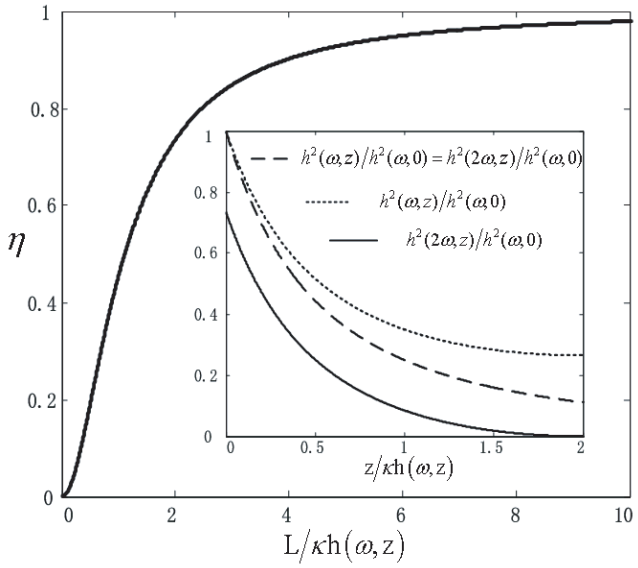

Figure 3. Main plot: Conversion coefficient η versus the normalized thickness of the slab. Inset: Transmission coefficient of fundamental wave (dotted curve) and reflection coefficient of second-harmonic wave (solid curve) versus $z/\kappa h(\omega, z)$ in the cases of $L/\kappa h(\omega, z) = 2$ and the complete conversion in a semi-infinite slab (dashed curve).

Seen from Fig. 3, the solid line of the main plot indicates transmission coefficient η of the fundamental wave converting into the second-harmonic wave versus the normalized slab thickness $L/\kappa h(\omega, z)$, $\eta = h^2(2\omega, 0)/h^2(\omega, 0)$. η increases as the slab thickness adds, and when $L \to \infty$, $\eta \to 1$. The insert plot shows the case of $L/\kappa h(\omega, z) = 2$, the dotted line denotes transmission coefficient of the fundamental wave $h^2(\omega, z)/h^2(\omega, 0)$ versus $z/\kappa h(\omega, z)$, the solid line denotes reflection coefficient of the

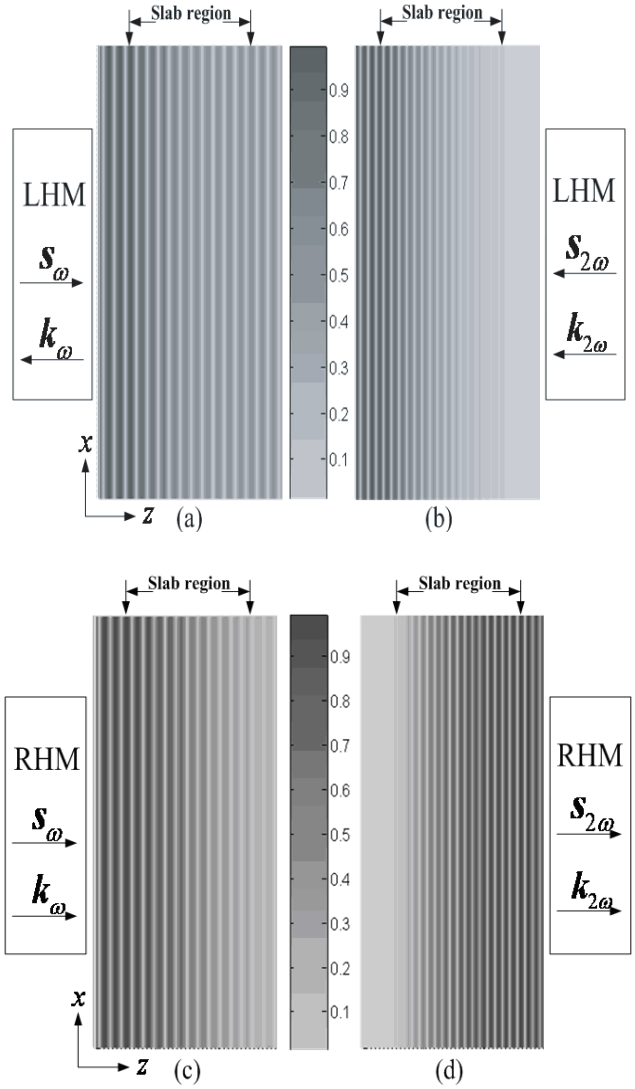

Figure 4. The comparison of the magnetic field intensity-distribution for the fundamental and the second-harmonic waves between a slab of LHM and a slab of RHM when the thicknesses are $L/\kappa h(\omega, z) = 2$. (a) Incident fundamental wave within and outside the LHM slab. (b) Reflected second-harmonic wave within and outside the LHM slab. (c) Incident fundamental wave within and outside the RHM slab. (d) Transmitted second-harmonic wave within and outside the RHM slab.

second-harmonic wave $h^2(2\omega, z)/h^2(\omega, 0)$ versus $z/\kappa h(\omega, z)$, the dashed line indicates the complete conversion in the case of semi-infinite slab, $h^2(\omega, z)/h^2(\omega, 0) = h^2(2\omega, z)/h^2(\omega, 0)$.

In order to observe the differences of the field distributions in nonlinear LHM and RHM slabs, we have computed propagating wave patterns for such slabs when the normalized slab thicknesses are $L/\kappa h(\omega, z) = 2$. Considering the LHM slab, we follow the mode of [10], $\varepsilon(\omega) = 1 - \omega_p^2/\omega^2$, $\mu(\omega) = 1 + F\omega^2/\omega_0^2 - \omega^2$, and take the other parameters of the composite: $f_0 = 5\,\text{GHz}$, $f_p = 7\,\text{GHz}$, $F = 0.3$, $a = 3\,\text{mm}$, $d = 6\,\text{mm}$, $U_c R_d = 1$, the exact phase-matching takes place at $f_F = 5.537\,\text{GHz}$. Fig. 4(a) shows the decreasing incident fundamental field intensity along the $-z$-axis in the slab-region, Fig. 4(b) shows the increasing reflected second-harmonic field intensity along the-axis, and the wave pattern of (b) is twice denser than that of (a). To keep the exact phase-matching condition in the RHM slab, we assume ε and μ are the absolute values of that of the LHM slab, and the other parameters are the same as the LHM slab. Fig. 4(c) shows the decreasing incident fundamental field intensity. Comparing Fig. 4(b) with Fig. 4(d), we can see second-harmonic wave in LHM slab propagates opposite to that in RHM slab.

4. SECOND-HARMONIC GENERATION UNDER PHASE-MISMATCHING CONDITION

Under phase-matching condition $\Delta k \neq 0$, equation (13) can also be solved in the small-signal approximation. We assume $dH(\omega, z)/dz \approx 0$, $H(\omega, z) = H(\omega, 0)$, then equation (4) can be written as:

$$dH(2\omega, z)/dz = j2\kappa H^2(\omega, 0)\exp(-j\Delta k z) \tag{17}$$

By the boundary condition $H(2\omega, L) = 0$, the magnetic field of the second-harmonic wave is the integral of (17):

$$H(2\omega, z) = -j2\kappa H^2(\omega, 0)\frac{2\sin[\Delta k(L-z)/2]\exp(-j\Delta k(L+z)/2)}{\Delta k} \tag{18}$$

The amplitude of the second-harmonic wave is:

$$h(2\omega, z) = 4\kappa h^2(\omega, 0)\left|\frac{\sin[\Delta k(L-z)/2]}{\Delta k}\right| \tag{19}$$

We note that under phase-mismatching condition, the amplitude of the second-harmonic wave oscillates between zero and maximum $4\kappa h^2(\omega, 0)/\Delta k$, the oscillation period is $T = \Delta k/4\pi$. The greater the

phase mismatched, the smaller the amplitude of the second-harmonics. This is the reason why we do not consider the higher order components in the second-harmonic generation in this paper. When the phase-matching condition is fulfilled, all other components are badly phase-mismatched, hence they provide no substantial contribution to the nonlinear parametric interaction.

5. CONCLUSIONS

Through an exact analysis, we have analyzed the second-harmonic response and the counter-propagating energy-flows in the lossless nonlinear LHM slabs beyond the constant-pump approximation. Firstly, based on the electromagnetic theory, the Manly-Rowe relations for nonlinear left-handed metamaterials are derived theoretically. Then, the basic coupled-mode equations in the small-signal approximation are obtained. The energy conversion process and spatial distribution of forward-propagating wave of fundamental frequency and backward-propagating wave of second harmonics under phase-matching condition are investigated. In particular, it is demonstrated that the surface of nonlinear LHM can operates as an effective mirror which reflects the energy in form of second harmonics. While numerical results of the comparison in the magnetic field intensity-distribution for the fundamental and the second-harmonic waves between a finite LHM slab and a finite RHM slab are given. Finally, the phase-matching condition is important to the investigation of nonlinear left-handed metamaterials which is illustrated from the angle of phase-mismatching. This work extends the nonlinear theory to the domain of LHM, and provides a basis to realize tunable nonlinear LHM.

ACKNOWLEDGMENT

This work is supported by the National Natural Science Foundation of China under contract no. 60601028.

REFERENCES

1. Veselago, V. G., "The electrodynamics of substances with simultaneously negative values of ε and μ," *Soviet Physics USPEKI*, Vol. 10, No. 4, 509–514, Jan.–Feb. 1968.
2. Pendry, J. B., "Negative refraction makes a perfect lens," *Physical Review Letters*, Vol. 85, No. 18, 3966–3969, Oct. 2000.

3. Smith, D. R. and N. Kroll, "Negative refraction index in left-handed materials," *Physical Review Letters*, Vol. 85, No. 14, 2933–2936, Oct. 2000.
4. Kong, J. A., "Electromagnetic wave interaction with stratified negative isotropic media," *Progress In Electromagnetics Research*, PIER 35, 1–52, 2002.
5. Liang, L., B. Li, S.-H. Liu, and C.-H. Liang, "A study of using the double negative structure to enhance the gain of rectangular waveguide antenna arrays," *Progress In Electromagnetics Research*, PIER 65, 275–286, 2006.
6. Li, B., B. Wu, and C.-H. Liang, "Study on high gain circular waveguide array antenna with metamaterial structure," *Progress In Electromagnetics Research*, PIER 60, 207–219, 2006.
7. Zharov, A. A., I. V. Shadrivov, and Yu. S. Kivshar, "Nonlinear properties of left-handed metamaterials," *Physical Review Letters*, Vol. 91, No. 3, 03740121–03740124, Mar. 2003.
8. Shadrivov, I. V., A. A. Zharov, N. A. Zharov, and Yu. S. Kivshar, "Nonlinear left-handed metamaterials," *Radio Science*, Vol. 40, RS3S90, 2005.
9. Zharov, A. A., N. A. Zharov, I. V. Shadrivov, and Yu. S. Kivshar, "Subwavelength imaging with opaque nonlinear left-handed lenses," *Applied Physics Letters*, Vol. 87, 091104, 2005.
10. Shadrivov, I. V., A. A. Zharov, and Yu. S. Kivshar, "Second-harmonic generation in nonlinear left-handed metamaterials," *Optical Society of America*, Vol. 23, No. 3, 529–534, Mar. 2006.
11. Manley, J. M. and H. E. Rowe, "General energy relations in nonlinear reactances," *Proc. IRE*, Vol. 47, 2115–2116, Dec. 1959.